Complex impedance analysis of $Ba_{0.65}Sr_{0.35}TiO_3$ ceramics

J. Jiang · T. J. Zhang · B. S. Zhang · H. Mao

Abstract Complex impedance spectra of BST ceramics were measured at different temperatures, and the results reveal that all the centers of the semicircles lie below the real axis, and the area of the semicircles decreases with the increasing temperature. Activation energy of grains and grain boundaries was obtained from a classical Arrhenius relation. The results show that the activation energy of grains and grain boundaries of undoped BST ceramics is 0.98 and 0.97 eV, respectively. After doping B_2O_3–SiO_2, the activation energy of grain increased to 1.12 eV, which was due to B_2O_3–SiO_2 redistribution to the grain boundary during the cooling process. The activation energy of grains increased to 1.16 eV after 1 mol% MgO doping, which was caused by the decrease of the oxygen vacancy concentration and the increase of the potential barrier of the grain boundary.

Keywords BST ceramics · Impedance spectra · Activation energy · Defect

1 Introduction

Barium strontium titanate ($Ba_{1-x}Sr_xTiO_3$) is one of the most promising condidates for applications in capacitors, infrared detectors, microwave devices and DRAMs due to its high

J. Jiang · T. J. Zhang (✉) · B. S. Zhang · H. Mao
Faculty of Materials Science and Engineering, Hubei University,
Wuhan 430062, People's Republic of China
e-mail: zhangtj@hubu.edu.cn

dielectric constant, low leakage current density, huge pyroelectric coefficient, and large tunability [1, 2].

It's well known that electrical properties of the poly-crystalline ceramics are strongly affected by their micro-structures [3, 4]. As a non-destructive analysis technique, an impedance spectrum that accurately reflects the micro-structure features is usually the best tool to analyze their electrical properties. In the complex impedance spectra of ideal polycrystalline ceramics, there are three semicircles [5, 6], as shown in Fig. 1(a), the first semicircle in the range of high frequency suggests the grain interior, the second semicircle in the range of middle frequency reflects the grain boundary effects, and the third semicircle in the range of low frequency reflects the ceramic-electrode interface effects. A semicircle of the AC data in the plane suggests an appropriate equivalent R-C circuit that represents the observed spectra. And the corresponding equivalent circuit of ideal polycrystalline ceramics was shown in Fig. 1(b), where $R_1=R_g$, $R_2=R_g+R_{gb}$, $R_3=R_g+R_{gb}+R_e$. However, there are only two semicircles reflecting the grain and the grain boundary effects in the impedance spectra when Ohmic electrode was used [7–13] or the measure frequency range isn't low enough. In this work, the impedance spectra measured from 100 Hz to 1 MHz at different temperature consist of two semicircles.

There are at least four possible defects in BST ceramics, namely, the interface defect at metal/ceramics Schottky junction, oxygen vacancies, barium vacancies and electron existing in the metal/BST/metal capacitors, which may lead to dielectric relaxation. Here, the important defects such as acceptor centers, doubly ionized oxygen vacancies $V_O^{..}$, electrons e' and holes $h^.$ are investigated. The possible
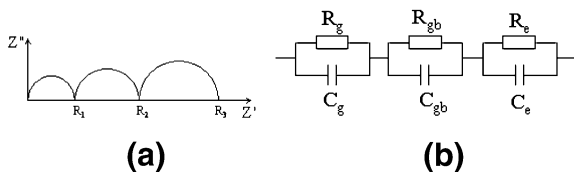
Fig. 1 Impedance spectra (a) and its equivalent circuit (b) of ideal polycrystalline ceramics

equilibrium reactions and their mass-action expressions are following [14, 15]:

$$O_O \rightleftharpoons \frac{1}{2} O_2 + V_O^{\cdot\cdot} + 2e' \qquad (1)$$

$$V_O^{\cdot\cdot} + \frac{1}{2} O_2 \rightleftharpoons O_O + 2h^{\cdot} \qquad (2)$$

In this paper, the change of the impedance spectra and the conductive mechanism were investigated.

2 Experiment

BST ceramics were prepared by a conventional solid-state reaction method. $BaCO_3$, $SrCO_3$, TiO_2, B_2O_3, SiO_2 and MgO were used as starting materials. The stoichiometric powders were mixed by ball-milling in agate mortars for 4 h, dried and calcined at 1000 °C for 2.5 h. The calcined aggregate were reball-milled and pressed into φ11×1.5 mm green pellets at a pressure of 200 MPa. The undoped, B_2O_3–SiO_2 doped and MgO doped green pellets were sintered at 1300, 1200 and 1300 °C for 2 h, respectively. Then the sintered specimens were polished to a thickness of 0.9 mm, electroded with silver paste and dried. The

impedance spectra of the specimens were measured with HP4192A LF impedance analyzer at different temperatures.

3 Results and discussion

3.1 Impedance spectra analysis

Figure 2 shows Impedance spectra of undoped BST ceramics measured at 290, 355 and 415 °C, respectively. It's obvious that all the centers of the semicircles lie below the real axis, and there is a depression angle caused by the oxygen vacancies in each semicircle, which indicates that the relaxation deviates from the ideal Debye relaxation mode. At the same time the area of the semicircle decreased with the increasing testing temperature, which indicates that the resistance of the grain (R_g) and the resistance of the grain boundary (R_{gb}) decreased. This decrease may be caused by the increase of the thermal movement of the defects, especially the oxygen vacancies [16].

Complex impedance of BST ceramics doped with 5 mol% B_2O_3–SiO_2 were measured at temperature from 240 to 660 °C is shown in Fig. 3. It's very clear that the dominant low frequency (LF) contribution completely overlapped the high frequency (HF) semicircle and showed only an arc when the measuring temperature is blow 331 °C. As the measuring temperature increased, R_g and R_{gb} showed the same decreasing trend for undoped BST ceramics. Furthermore, at higher frequency the inductive contribution from the platinum lead wires is not neglectable. So R_{gb} deceased continuously with temperature and finally merged with R_g. It indicates that for BST ceramics doped with 5 mol%B_2O_3–SiO_2, the effects of the grain boundary enhanced, which was due to the decrease of the grain size and the increase of the insulator volume fraction of the grain boundary in per unit cell.

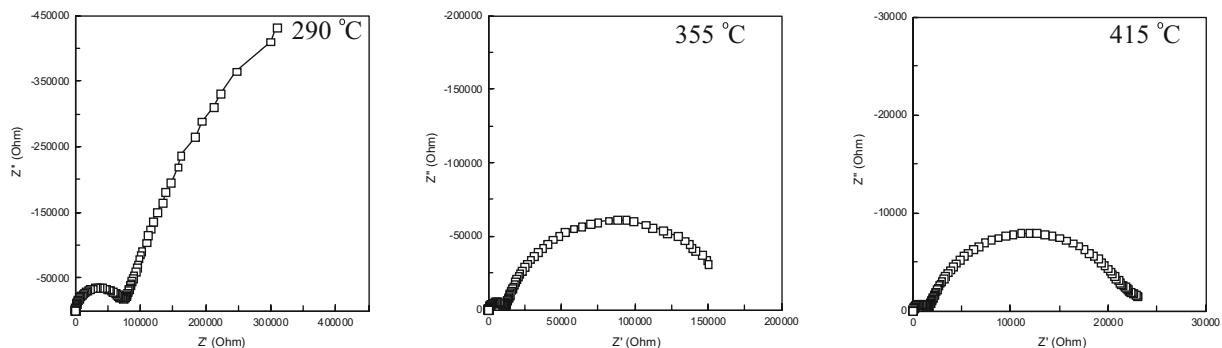As Daniels et al. suggested previously, the grain boundary could be oxidized and generate the neutral barium

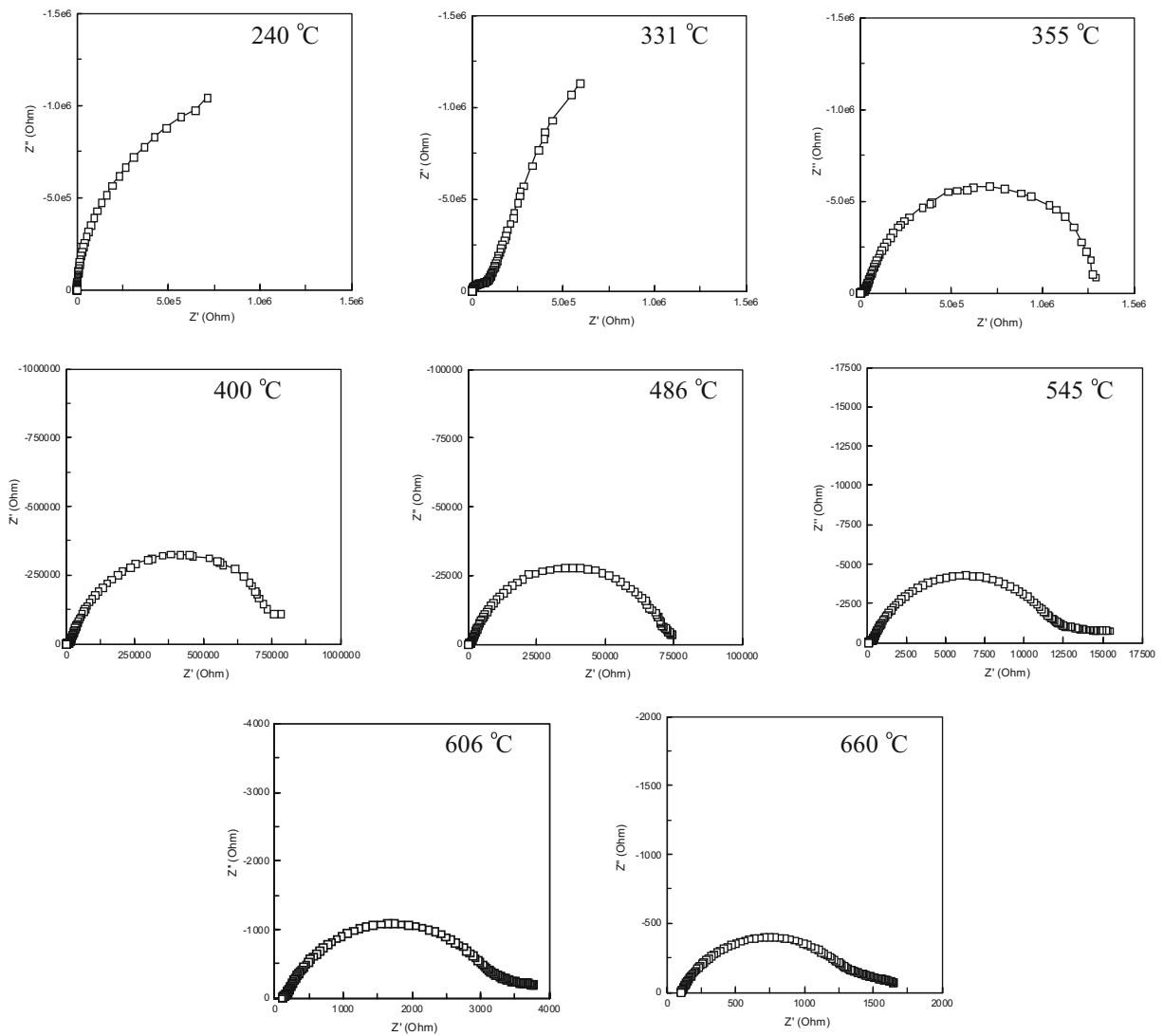Fig. 2 Impedance spectra of BST ceramics at different temperature

Fig. 3 Impedance spectra of 5 mol% B_2O_3–SiO_2 doped BST ceramics at different temperature

Fig. 4 An Arrhenius plots of lnσ vs. 1000/T. (where E_{ag} denotes the activation energy of the grains, E_{agb} denotes the activation energy of the grain boundaries). (a) Activation energy of the grain is 0.98 eV; (b) activation energy of the grain is increased to 1.12 eV
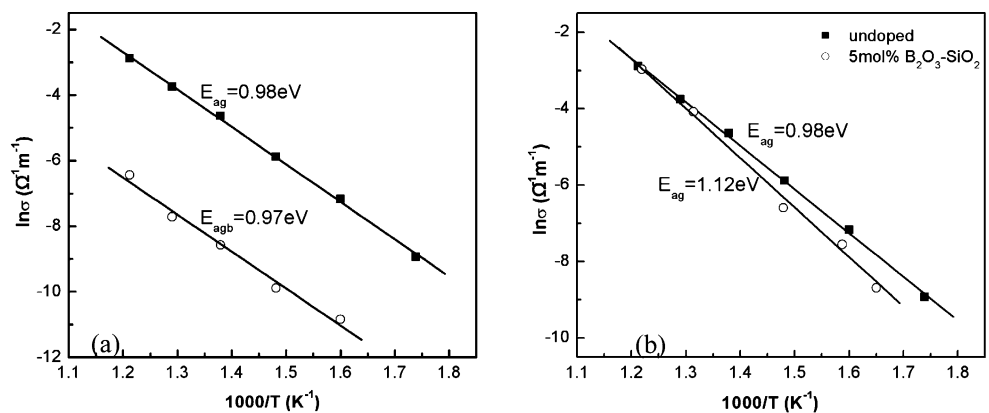
vacancy, and the defect chemistry reaction can be expressed as following [17, 18]

$$\frac{1}{2} O_2 \rightarrow V_{Ba}^{\times} + O_O^{\times} \tag{3}$$

The neutral barium vacancy at grain boundary can capture the free electron to be ionized, and the reaction is

$$V_{Ba}^{\times\times} + 2e' \rightarrow V_{Ba}'' \tag{4}$$

For BST ceramics doped with B_2O_3–SiO_2, small part of the dopants vaporized during the sintering, and most of the dopants remained in the grain boundary during the cooling process in air [19]. So the defect chemistry reaction below occurred easily in the grain boundary.

$$B_2O_3 + V_{Ba}^{\times} \rightarrow 2B_{Ba}^{\cdot} + V_{Ba}'' + 2O_O^{\times} + \frac{1}{2} O_2(g) \tag{5}$$
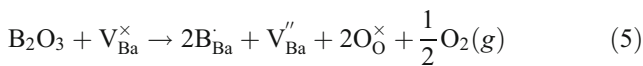
Then V_{Ba}'' became the main carrier in BST ceramics doped with B_2O_3–SiO_2, and the conductivity increased with the increase of temperature, so R_{gb} decreased.

3.2 Activation energy analysis

Conductivity of BST ceramics can be expressed as a classical Arrhenius relation below [1, 2].

$$\sigma = \sigma_0 \exp\left(\frac{-E_a}{kT}\right) \tag{6}$$

Where E_a is activation energy, k is the Boltzmann constant, and T is the measuring temperature. On the basis of Eq. 6, E_a can be obtained from the slopes of the linear regions of the plots $\ln\sigma$ vs. $10^3/T$.

Figure 4 shows the modified Arrhenius curve of undoped BST ceramics. In Fig. 4(a), activation energy of the grain (E_{ag}) and the grain boundary (E_{agb}) of undoped BST ceramics is 0.98 and 0.97 eV, respectively. After doping 5 mol%B_2O_3–SiO_2, the activation energy of the grain increased to 1.12 eV, as shown in Fig. 4(b). It's well known that the carriers must penetrate into the grain boundary when they move in the ceramics. The ratio of the grain boundary increased after doping, so E_{ag} increased.

Table 1 Activation energy of BST ceramics doped with MgO.

MgO content	0 mol%	0.5 mol%	1.0 mol%	1.5 mol%	2.0 mol%
E_{ag}(eV)	0.98	1.04	1.16	1.14	1.12

Activation energies of BST ceramics doped with different MgO content were listed in Table 1. It can be seen that E_{ag} increased after doping MgO. It's well known that MgO is an acceptor for BST ceramics, and the radius of Mg^{2+}(0.65 Å) is smaller than that of Ti^{4+}(0.68 Å). When replacing Ti^{4+}, Mg^{2+} prevent the reduction of Ti^{4+} to Ti^{3+} by neutralizing the donor action of the oxygen vacancies [20, 21]. Then the concentration of the oxygen vacancy in BST ceramics decreased, and E_{ag} increased. It's very clear that when MgO content reaches 1 mol% the maximum activation energy was 1.16 eV, and this revealed that the deep energy level of acceptor was located at 1.16 eV above the top of valence band of BST ceramics, which was determined from the known band-gap of BST (3.5 eV) [1, 2]. In summary, activation energy increased after doping B_2O_3–SiO_2 and MgO, though the mechanism is different.

4 Conclusions

BST ceramics were prepared by a conventional solid-state reaction method. Complex impedance of the ceramics measured at different temperature showed that all the centers of the semicircles lie below the real axis, and the area of the semicircle decreased with the increasing test temperature. The activation energy of grain and grain boundary of undoped BST ceramics is 0.98 and 0.97 eV, respectively. After doping B_2O_3–SiO_2, the activation energy of grain increased to 1.12 eV, which was due to B_2O_3–SiO_2 redistribution to the grain boundary during the cooling process. The activation energy of grain also increased after doping MgO, but the mechanism is due to decrease the concentration of the oxygen vacancy and enhance the potential barrier. When doping content reaches 1 mol% MgO, the activation energy is 1.16 eV, which indicates that energy level of MgO acceptor was located at 1.16 eV above the top of valence band of BST ceramics.

References

1. M.S. Tsai, T. Ytseng, Mater. Chem. Phys. **57**, 47 (1998)
2. Y.-P. Wang, T.-Y. Tseng, Thin Solid Films **346**, 269 (1999)
3. G. Senthil Murugan, K.B.R. Varma, J. Electroceramics **8**, 37 (2002)
4. L. Yuh-Yih, T.-Y. Tseng, Mater. Chem. Phys. **53**, 132 (1998)
5. Z. Tianjin, W. Yong, J. Hubei University (Natural Science Edition), **21**, 134 (1999)
6. R .K. Dwivedi, D. Kumar, O. Parkash, J. Mater. Sci. **36**, 3657 (2001)
7. Y. Wu, M.J. Forbess, S. Seraji, et al., Mater. Sci. Eng. **B86**, 70 (2001)
8. T. Xiaofeng, T. Zilong, Z. Zhigang, J. Inorg. Mater. **15**(6), 1037 (2000)
9. D. Huiling, W. Guomei, L. Jiaheng, J. Func. Mater. **28**(5), 495 (1997)
10. N.S. Hari, P. Padmini, T.R.N. Kutty, J. Mater. Sci., Mater. Electron. **8**, 15 (1997)
11. A.R. West, D.C. Sinclair, et al., J. Electroceramics **1**(1), 65 (1997)
12. E.J. Abram, K.C. Sinclair, A.R. West, J. Electronceramics **10**, 165 (2003)
13. S. Rodewald, J. Fleig, J. Maier, J. Eur. Ceram. Soc. **21**, 1749 (2001)
14. D.M. Smyth, J. Electroceramics **11**, 89 (2003)
15. M. Bollmann, R. Waser, J. Electronceramics **1**(1), 51 (1997)
16. M. Dawber, J.F. Scott, A.J. Harmann, J. Eur. Ceram. Soc. **21**, 1633 (2001)
17. J. Qi, Z. Gui, Y. Wang, et al., Mater. Sci. Eng. **B95**, 283 (2002)
18. Z. Zhongtai, M. Qing, S. Hongfei, J. Func. Mater. **29**(4), 366 (1998)
19. S.H. Yoon, H. Kim, J. Eur.Ceram. Soc. **22**, 689 (2002)
20. B. Su, T.W. Button, J. Appl. Phys. **95**(3), 1382 (2004)
21. P.C. Joshi, M.W. Cole, Appl. Phys. Lett. **77**(2), 289 (2000)